TECHNICAL BRIEF

Evaluation of microarray surfaces and arraying parameters for autoantibody profiling

Imelda Balboni[1, 2], Cindy Limb[1], Jessica D. Tenenbaum and Paul J. Utz[1, 3]*

[1] Department of Medicine, Division of Immunology and Rheumatology, Stanford University, Stanford, CA, USA
[2] Department of Pediatrics, Division of Rheumatology, Stanford University, Stanford, CA, USA
[3] Department of Medicine, Stanford Biomedical Informatics, Stanford University, Stanford, CA, USA

Autoantigen microarrays are being used increasingly to study autoimmunity. Significant variation has been observed when comparing microarray surfaces, printing methods, and probing conditions. In the present study, 24 surfaces and several arraying parameters were analyzed using >500 feature autoantigen microarrays printed with quill pins. A small subset of slides, including FAST®, PATH®, and SuperEpoxy2, performed well while maintaining the sensitivity and specificity of autoantigen microarrays previously demonstrated by our laboratory. By optimizing the major variables in our autoantigen microarray platform, subtle differences in serum samples can be identified that will shed light on disease pathogenesis.

Received: February 14, 2008
Revised: April 9, 2008
Accepted: May 1, 2008

Keywords:
Autoantibody profiling / Autoantigens / Autoimmune disease / Multiplexed proteomics technology / Protein microarrays

Autoantigen microarray technology enables the comprehensive analysis of autoantibodies directed against hundreds of antigens including proteins, peptides, nucleic acids, lipids, and macromolecular complexes, with microliter volumes of serum in a high-throughput manner (reviewed in ref. [1]). Initial studies demonstrated that autoantigen microarrays are both sensitive and specific for detecting autoantigens using human sera [2], and since then autoantigen microarrays have been used to study autoimmune diseases and their animal models including systemic lupus erythematosus [2–5], rheumatoid arthritis [2, 3, 6, 7], type I diabetes [8], and multiple sclerosis [9, 10].

Given the heterogeneous nature of proteins, optimal conditions for autoantigen microarrays have not been established, and variation has been observed using different slide surfaces, printing methods, and arraying conditions. Initial autoantigen microarray studies utilized poly-L-lysine-coated slides designed for DNA microarrays [2]. While this worked for many proteins and peptides, some antigens were not detectable, most likely related to structural changes, steric interference, or charge [2]. Subsequent studies have used poly-L-lysine [4, 6, 9], SuperEpoxy or SuperEpoxy2 [6–8], SuperAldehyde [4], Hydrogel™ [4], and FAST® slides [5, 11, 12], as well as polystyrene wells [3]. Angenendt *et al.* [13] evaluated several surfaces for protein microarrays including amine, epoxy, silanated, FAST, polystyrene, PEG-Epoxy, and dendrimer slides for signal-to-spotted concentration ratios, LODs, and CV. CVs ranged from 16 to 40% for different surfaces, with poly-L-lysine having the best CV of 16% [13]. The results of this study cannot be generalized to all autoantigen microarray studies as the protein was printed with solid pins while autoantigen microarrays printed in our laboratory and several others utilize quill pins [2, 6, 7, 9]. Several studies do not report which type of pin was used [4, 5], and others have utilized ink jet printers [3]. In addition, Angenendt's study evaluated only one protein, HSA, probed with a mAb against

Correspondence: Dr. Imelda Balboni, Stanford University, Department of Medicine, 269 Campus Dr. CCSR 2250, Stanford, CA 94305, USA
E-mail: mbalboni@stanford.edu
Fax: +1-650-723-7509

Abbreviations: B/B′, U-snRNP Protein B/B′; **CPI,** composite pixel intensity; **GAH,** goat anti-human; **GAM,** goat anti-mouse; **his-tag,** hexa-histidine purification tag; **MFI-B,** median fluorescence intensity minus background; **Ribo P,** ribosomal phosphoprotein P; **U1-A,** U1-snRNP A Protein

* Current address: Duke Translational Medicine Institute, Duke University, Durham, NC, USA

HSA, and thus may not be applicable to autoantigen microarrays printed with hundreds of antigens and probed with polyclonal sera. A major interest of our laboratory is to use autoantigen microarrays to follow autoantibody responses within a patient over time, where subtle differences need to be detected. Therefore, we sought to determine optimal conditions for printing autoantigen microarrays based on our initial studies demonstrating their utility in studying connective tissue diseases [2].

Autoantigen microarrays were generated by spotting distinct antigens in replicate sets using a robotic microarrayer as previously described [14]. A complete list of autoantigens used for these studies, including their manufacturer, origin, and common disease associations, is shown in the Supporting Information (Table S1). Autoantigens were diluted in PBS at various concentrations, transferred into 384-well plates and spotted onto microarray slide surfaces in an ordered array. The initial screens were performed using microarrays printed with a robotic microarrayer manufactured according to the specifications listed on the website of Patrick Brown's Laboratory at Stanford University (http://cmgm.stanford.edu/pbrown/mguide/index.html) with ChipMaker 2 Micro-Spotting Pins (TeleChem International, Sunnyvale, CA, USA). Subsequent studies were performed using a VersArray ChipWriter Pro microarrayer (BioRad Laboratories, Hercules, CA, USA) with a customized printhead and Silicon Microarray™ Spotting Pins (Parallel Synthesis Technologies, Santa Clara, CA, USA).

Prior to probing, microarrays were blocked overnight at 4°C in a blocking buffer solution of PBS with 0.5% TWEEN®20 and 3% FCS. Blocked microarrays were removed, excess fluid was drained, and microarrays were immediately placed in histology chambers where probe solution was added. Microarrays were incubated for 1 h at 4°C with dilutions of a histidine-specific (hexa-histidine purification tag, his-tag) His-Tag® mAb (Novagen, San Diego, CA, USA) in PBS with 3% FCS, rinsed briefly and washed twice for 20 min in blocking buffer. Microarrays were then incubated with a 1:2000 dilution of Cy™3- or Cy™5-conjugated AffiniPure goat antimouse (GAM) IgG and IgM (H&L) secondary antibody with minimal crossreaction to human, bovine, and horse serum proteins (Jackson ImmunoResearch Laboratories, West Grove, PA, USA) in PBS with 3% FCS for 1 h at 4°C, rinsed, and washed twice in blocking buffer for 30 min, twice in PBS for 20 min, and twice in deionized water for approximately 30 s. Microarrays were spun dry and scanned using a GenePix™ 4000 Scanner (Molecular Devices Corporation, Sunnyvale, CA, USA). Digital images were collected and stored in a database for subsequent analysis. Similar studies were performed using human positive control sera (ImmunoVision, Springdale, AR, USA) and Cy3-conjugated AffiniPure goat antihuman (GAH) IgG and IgM (H&L) secondary antibody with minimal crossreaction to bovine serum proteins (Jackson ImmunoResearch Laboratories).

Quantitative analysis of the fluorescence intensity of individual features was performed using GenePix Pro 6.0 software (Molecular Devices Corporation). The location of each antigen feature was identified using the GenePix Pro proprietary feature-finding algorithm for irregular features, and the median fluorescence intensity minus background (MFI-B) of each feature was determined, based on the median pixel intensity within the circumscribed antigen feature minus the background, represented by the median pixel intensity in the surrounding local area. After applying the feature-finding algorithm, each feature was inspected and the feature adjusted manually if indicated. Features deemed unsuitable due to significant background or poor printing were excluded from the data analysis. Descriptive statistics were calculated for replicate features for each antigen on the microarrays to determine median MFI-B, CV within a microarray (intraslide CV) and among microarrays (interslide CV), and S/N. CV was calculated as (SD/mean)100 of the MFI-B, and S/N calculated as (MFI-B)/(SD of background).

We analyzed 22 commercially available slide surfaces for overall background, uniformity, streaking, and smearing of features (Table 1). Many slide surfaces did not have specific protocols recommended for printing and probing microarrays although some manufacturers, including Whatman, Sigma (for SigmaScreen™ APS slide), and ArrayIt®, recommended the use of proprietary print, block, and/or wash buffers. The initial screens of microarray surfaces were performed using the protocol established for autoantigen microarrays by Robinson *et al.* [2] without the use of these proprietary solutions. However, given the significant differences in protocol, CodeLink™ Activated slides were processed according to the manufacturer's protocol. For these screens, five slides of each type were tested and slide order was permuted in a nonrandom fashion to eliminate bias due to slide placement. A 726-feature microarray was fabricated with ten autoantigens at 200 μg/mL, and ten different Cy5- or Alexa Fluor® 647-labeled "dopes," printed alone and in combination with each other, in replicates of six. Cy3 and Cy5 dyes were spotted to orient the arrays. Slides were probed with a His-Tag mAb (Novagen) and Cy3-conjugated GAM IgG and IgM (Jackson ImmunoResearch Laboratories).

Representative images from the initial screens are shown in the Supporting Information (Fig. S1A). Slides that were suitable, based on visual inspection and a coated printing surface of at least 16 mm × 40 mm, were chosen for further evaluation. Of the slides evaluated, all except for HydroGel slides met this size requirement. Ten surfaces (Table 1, footnote a) were retested to confirm suitability and to determine CVs. For this round of screening, a 608-feature microarray was fabricated including six antigens and several dopes at different concentrations, printed in replicates of eight. Specific conditions recommended by slide manufacturers were followed for probing these microarrays. CVs of these ten surfaces are shown in the Supporting Information (Fig. S2). A cutoff of less than 30% was set for both intraslide and

Table 1. Slide surfaces evaluated for printing autoantigen microarrays

Slide	Manufacturer	Surface coating	Intended use
[a)]FAST	Whatman	NC-based polymer	Protein microarrays
[b)]PATH	GenTel® BioSciences	Ultra-thin NC	Protein microarrays
Protein Glass	NUNC	Modified polymer	Protein microarrays
Low Background Aldehyde	MicroSurfaces	Aldehyde monolayer	Protein, peptide, antibody arrays
HydroGel	Perkin Elmer	Acrylamide-based polymer	Protein microarrays
[a)]Zeta-Grip™ Chips	Miragene	Hydrophobic polymer	Protein microarrays
[a)]CodeLink Activated Slides	Amersham	Hydrophilic, amine reactive polymer	Amine binding
[a)]SuperProtein	ArrayIt	Hydrophobic polymer	Protein microarrays
[a)]SuperEpoxy	ArrayIt	Epoxide groups	Oligonucleotide, cDNA, protein, cell, tissue arrays
[b)]SuperEpoxy2	ArrayIt	Epoxide groups	Oligonucleotide, cDNA, protein, cell, tissue arrays
SuperAldehyde	ArrayIt	Primary aldehyde groups	Oligonucleotide, cDNA, protein, cell, tissue arrays
[a)]SuperNitro	ArrayIt	NC	Protein microarrays
[a)]Poly-L-lysine	CEL Associates	Poly-L-lysine	DNA microarrays
[a)]Acrylic	CEL Associates	Acrylic amine	DNA microarrays
Hydrazine	CEL Associates	Hydrazine	DNA microarrays
Mercapto	CEL Associates	Mercapto silane	DNA microarrays
Epoxy	CEL Associates	Epoxide groups	DNA microarrays
Amine	CEL Associates	3-Aminopropyl groups	DNA microarrays
Carboxyl	CEL Associates	Carboxyl groups	DNA microarrays
Silylated (aldehyde)	CEL Associates	Reactive aldehyde groups	*In situ* hybridization, immunohistochemistry, DNA
[a)]Silanated (amine)	CEL Associates	Amine reactive groups	*In situ* hybridization, immunohistochemistry
Aldehyde	CEL Associates	Reactive Aldehyde groups	Oligonucleotide microarrays
[a)]Silane-Prep	Sigma	Aminoalkylsilane	*In vitro* diagnostic use
SigmaScreen APS	Sigma	Aminopropylsilane	DNA microarrays

a) Slides passed the initial screen and evaluated for CV.
b) Slides tested after initial screens had been performed.

interslide CVs to consider a slide suitable for further study. In addition, slides were inspected visually to ensure that the majority of features printed well on the slides. Based on these guidelines, FAST and poly-L-lysine slides were considered suitable, with intraslide and interslide CVs less than 30% and minimal streaking and smearing of features. Although SuperEpoxy slides did not meet the criteria, we included these slides in an additional study since they had been used in several of the autoantigen microarray studies published to date [2, 4, 6–9]. However, the subsequent study with poly-L-lysine and SuperEpoxy slides demonstrated that many antigens did not spot well on these surfaces, leading to background streaking and smearing of some antigens and no adherence for others. Data from this study are shown in Fig. 1C and of the Supporting Information (Fig. S3). However, based on these results, poly-L-lysine and SuperEpoxy slides were not included in most of the analyses presented below.

Two additional surfaces, SuperEpoxy2 and PATH® protein microarray slides, became available after the initial studies had been performed. These surfaces were subsequently tested alongside the FAST surface for a direct comparison. For this study, a 696-feature microarray was printed including U1-snRNP A Protein (U1-A) and U-snRNP Protein B/B′ (B/B′) (Diarect AG, Freiburg, Germany) at 50, 100, 200, and 400 μg/mL, and approximately 50 other antigens at 200 μg/mL and capture antibodies at 2–50 μg/mL (listed in Table S1). Antigens were printed in replicates of eight, and six slides of each surface were probed with the His-Tag mAb (Novagen) and Cy3-conjugated GAM IgG and IgM (Jackson ImmunoResearch Laboratories). The PATH slides were processed using reagents specific for this surface, following the manufacturer's protocol.

CVs for FAST, PATH, and SuperEpoxy2 slides were calculated for 18 his-tagged antigens printed at 200 μg/mL. Overall, FAST slides had the lowest CVs, with an intraslide CV as low as 3.5% (Fig. 1A, PM/Scl 100) and an interslide CV as low as 6.0% (Fig. 1B, B/B′). The median intraslide and interslide CVs were 7.6 and 10.5% for FAST slides; 12.3 and 17.8% for PATH slides; and 9.0 and 12.9% for SuperEpoxy2 slides, respectively (Figs. 1A and B).

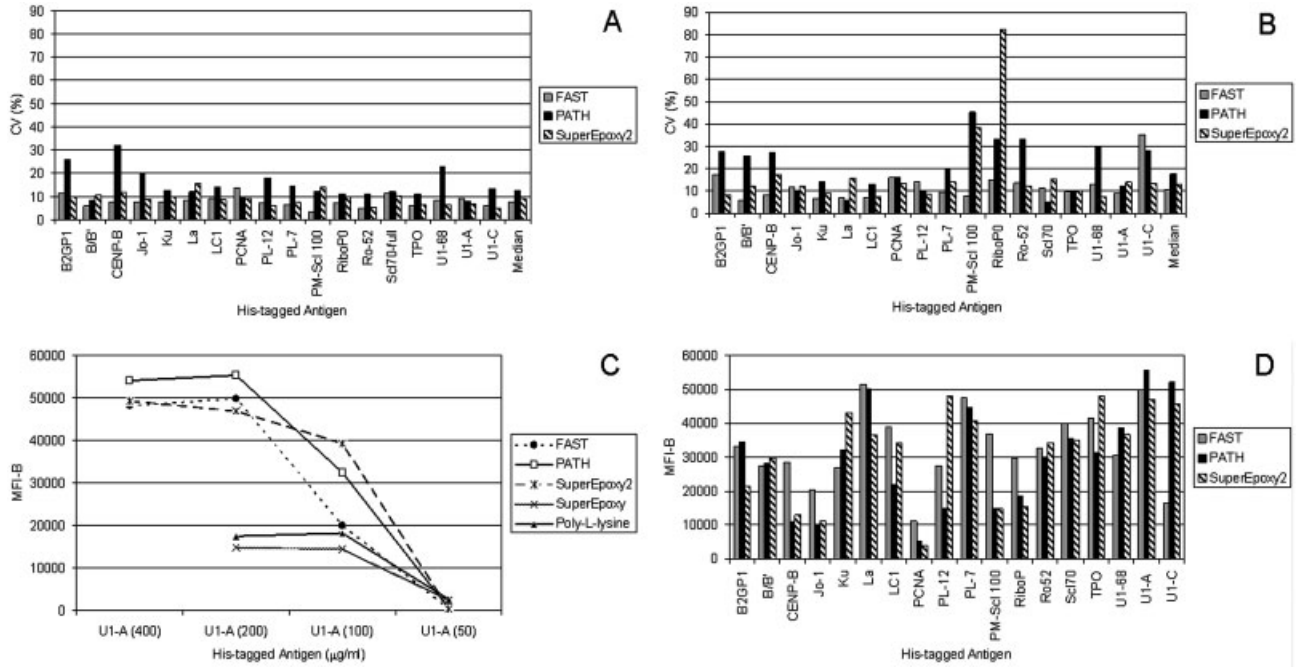

Figure 1. Autoantigen microarray analysis using a histidine-specific mAb. (A) Intraslide CVs and (B) interslide CVs were compared for a panel of recombinant human his-tagged antigens printed on FAST, PATH, and SuperEpoxy2 slides at 200 μg/mL using a robotic microarrayer. (C) MFI-Bs were compared for U1-A on FAST, PATH, SuperEpoxy2, SuperEpoxy, and poly-L-lysine slides printed at 400, 200, 100, and 50 μg/mL. (D) MFI-Bs were compared for a panel of recombinant human his-tagged antigens printed at 200 μg/mL on FAST, PATH, and SuperEpoxy2 slides. Six microarrays of each slide surface were probed with a histidine-specific His-Tag mAb (Novagen®) and Cy3-conjugated GAM IgG and IgM secondary antibody (Jackson ImmunoResearch Laboratories). For (A), the CV for each antigen was calculated from eight replicate features on each slide, and the median intraslide CV for six slides was calculated for each antigen. For (B), the median MFI-B for each antigen was calculated from eight replicate features on each slide, and the interslide CV among six slides was calculated. The "median" data points represent the median of CVs for all 18 his-tagged antigens for each surface. For (C) and (D), each data point represents the median MFI-B of 48 features calculated from eight replicate features on six slides of each surface. CV = (SD/mean)100 of the MFI-B β2GP1, β2 glycoprotein 1; CENP-B, centromere protein B; Jo-1, histidyl-tRNA synthetase; Ku, Ku (p70/p80); La, La/SS-B; LC1, liver cytosol type I-antigen; PCNA, proliferating cell nuclear antigen; PL-12, alanyl-tRNA synthetase; PL-7, threonyl-tRNA synthetase; Ribo P, ribosomal phosphoprotein P0; Ro52, Ro/SS-A 52 kDa; Scl-70, DNA topoisomerase I; TPO, thyroid peroxidase; U1-68, U1-snRNP-68 protein; U1-A, U1-snRNP-A protein; U1-C, U1-snRNP-C protein.

MFI-B increased for antigens printed on FAST, PATH, and SuperEpoxy2 slides at concentrations from 50 to 200 μg/mL and then plateaued (Fig. 1C). Based on this finding, we currently fabricate microarrays with antigens at a concentration of 200 μg/mL, except for capture antibodies, which are printed at concentrations between 2 and 50 μg/mL. The original SuperEpoxy and poly-L-lysine slides are no longer manufactured and could not be retested in a side-by-side comparison to PATH and SuperEpoxy2 slides. Therefore, Fig. 1C shows MFI-B of poly-L-lysine and SuperEpoxy slides from an earlier study. At a concentration of 400 μg/mL, U1-A could not be analyzed on the poly-L-lysine or SuperEpoxy slides due to significant background and smearing of the features, suggesting the surfaces were overloaded at that concentration, yet both had significantly lower MFI-B at 200 μg/mL compared to FAST, PATH, and SuperEpoxy2 slides (Fig. 1C).

Analysis of the MFI-B for the panel of his-tagged antigens demonstrated variability in the MFI-B among antigens and slide surfaces, suggesting that distinct antigens deposit differently on the various slide surfaces (Fig. 1D). This is likely due to the heterogeneous nature of the proteins and differences in the surface properties of the slides. We have calculated CVs of the background for the slide surfaces analyzed above (data not shown). CVs of the background of FAST, PATH, and SuperEpoxy2 slides were consistently low, with medians ranging from 4 to 7%. However, the CVs of the background for the other nine slides discussed in Fig. S2 were more variable, with medians ranging from 6 to 60%. This suggests that the sources of variability are multiple, and their relative contribution to the overall CV may be different for different slide surfaces.

Other probing, scanning and gridding parameters were also evaluated. No significant differences in MFI-B or CV were found when comparing Cy3 and Cy5-conjugated secondary antibodies or by adjusting the focus position of the scanner when scanning the microarrays (data not shown). The composite pixel intensity (CPI) threshold is a setting used when gridding microarrays to determine which pixels

are included in a feature during alignment. The spot-finding algorithm excludes pixels with intensities lower than the CPI threshold, unless it is surrounded by brighter pixels. We have compared intraslide and interslide CVs for his-tagged antigens after gridding the microarrays with a CPI threshold of 1000, 100, 10, and zero. Interestingly, while the CVs for most antigens were not affected by the CPI threshold, the CVs for a few antigens increased significantly with the lower CPI threshold (data not shown). This is likely secondary to properties of the antigens that affect how they deposit on the microarray surface.

Human positive control sera (ImmunoVision) with known reactivity to several autoantigens present on our autoantigen microarrays were used to further evaluate the FAST, PATH, and SuperEpoxy2 slides. Six hundred ninty-six-feature microarrays were fabricated and processed as described above, and probed with sera diluted 1:300 in PBS with 3% FCS, and Cy3-conjugated GAH IgG and IgM (Jackson ImmunoResearch Laboratories). Intraslide CVs for FAST slides were most consistent, ranging from 3.7 to 20.5%, with a median of 9.3% (Fig. 2A). The intraslide CVs for PATH and SuperEpoxy2 slides were more variable, with ranges of 5.0–44.3% and 3.5–53.5%, respectively, and medians of 11.3 and 17.7%, respectively (Fig. 2A).

LOD was estimated by probing with ribosomal phosphoprotein P (ribo P)-reactive serum at several dilutions. The MFI-B for the ribo P antigen decreased linearly from titers of 1:75 to 1:1200 on the FAST slide (Fig. 2B). Reactivity to other antigens was also detected, reflecting other expected autoreactivity and previous immunization against tetanus in this polyclonal patient sample (Fig. 2B). PATH slides performed similarly, while the MFI-B plateaued at 1:300 on the SuperEpoxy2 slide (data not shown). No reactivity was detected on microarrays probed with ribo P-reactive serum at a dilution of 1:75 without secondary antibody, or on microarrays probed with buffer instead of ribo P-reactive serum (Fig. 2B). Although we did not dilute the sera further to establish the precise LOD, these studies show that the LOD for each slide is at least 1:1200, which is well within the range of dilutions used for routine clinical measurement of autoantibodies in serum.

Nonspecific binding and crossreactivity were evaluated for FAST, PATH, and SuperEpoxy2 slides in the experiments discussed above by including the following control microarrays: (i) probed without a primary or secondary antibody, (ii) probed with a primary antibody (either His-Tag mAb or human ribo P-specific serum) but without a secondary antibody, and (iii) probed without a primary antibody but with a Cy3-conjugated secondary antibody (either GAH or GAM IgG and IgM). In addition, we calculated MFI-B for non-his-tagged antigens on microarrays probed with the His-Tag mAb and Cy3-conjugated GAM IgG and IgM, which would not be expected to fluoresce. To address nonspecific binding of human serum, we calculated MFI-B for antigens not expected to fluoresce on microarrays probed with the ribo P-specific positive control serum and Cy3-conjugated GAH IgG and IgM. Ribo P, GRP78, ssDNA, tetanus, and histones were excluded from this analysis based on the results shown in Fig. 2B. Summary statistics for these analyses are shown in the Supporting Information (Table S2). Similar results were observed when thyroid peroxidase was excluded from the analysis of microarrays probed with thyroid peroxidase-specific human positive control serum and Cy3-conjugated GAH IgG and IgM (data not shown). All three surfaces performed well in these analyses, without significant nonspecific binding or crossreactivity.

S/N was calculated for FAST, PATH, and SuperEpoxy2 slides probed with the His-Tag mAb and human positive control sera. Results from these analyses are shown in the Supporting Information (Table S3). For arrays probed with the His-Tag mAb and human positive control sera, SuperEpoxy2 slides had the lowest mean and median S/N, while PATH slides had the highest mean S/N and FAST slides had the highest median S/N (Table S3). The discrepancy between the highest mean and median values is due to the larger asymmetry of distribution around the mean, or increased skew, for PATH slide S/N compared to FAST slide S/N. Overall, the S/Ns for all three slides were well above the level expected to reliably detect a positive signal.

Given the potential variability among microarray features, we evaluated a method of "doping in" a fluorescently labeled molecule with each printed antigen to normalize features among microarrays to the doped molecule. We initially tested several conjugated molecules including ovalbumin, BSA, streptavidin, biotin, and two peptides, as well as Cy5 (Amersham Biosciences, Pittsburg, PA, USA) and Alexa Fluor 647 (Invitrogen™) dye alone. We further evaluated various concentrations of Alexa Fluor 647 doped into the antigens but did not find this to be a useful method for normalization as there was no improvement in CVs and no difference in relative fluorescence with doping (data not shown). We also printed microarrays with antigen solutions containing TWEEN20 and found this did not improve CV (data not shown). Finally, using human positive control sera and the his-tagged mAb, we compared microarrays printed and probed on different days. Interslide CVs for slides printed on the same day and probed on different days, and for slides printed on different days and probed on the same day were similar to those obtained in the studies presented above (data not shown), suggesting there is not significant variability among microarrays printed on different days or probed on different days.

Since these studies were undertaken, additional surfaces have likely become available that may also be appropriate for printing autoantigen microarrays. In addition, some slide surfaces that were not analyzed in detail may be useful for specialized analyses, or printing of peptides or other biomolecules. Although beyond the scope of this paper, it is also possible that careful protocol optimization for individual slide chemistries or utilization of a different pin type to fabricate the arrays may improve slide performance. Interestingly, Angenendt *et al.* [13] found poly-L-lysine slides per-

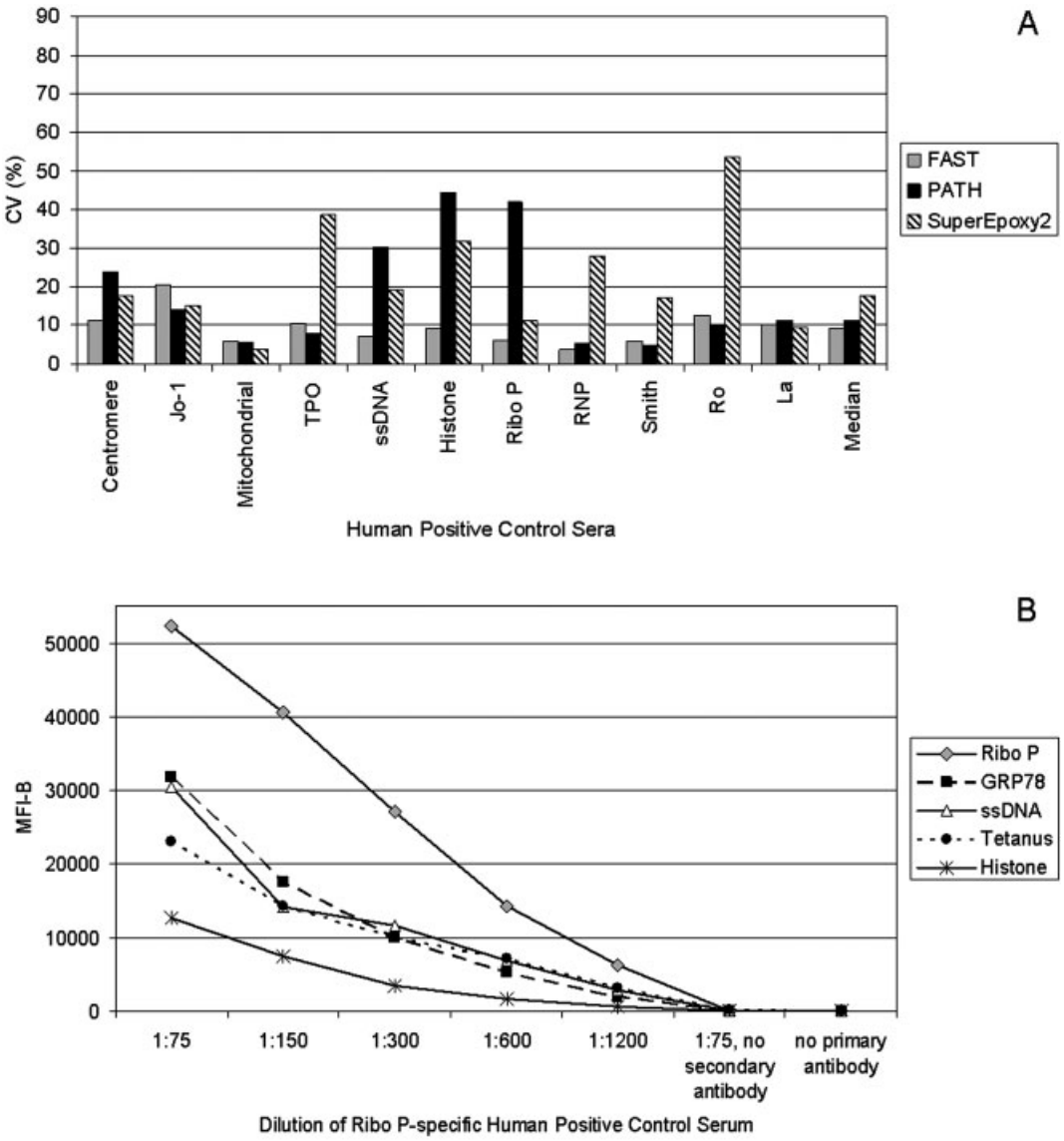

Figure 2. Autoantigen microarray analysis using human positive control sera. Autoantigens were printed on FAST, PATH, and SuperEpoxy2 slides using a robotic microarrayer, probed with human positive control sera (ImmunoVision) and Cy3-conjugated GAH IgG and IgM secondary antibody (Jackson ImmunoResearch Laboratories). (A) Intraslide CVs for each serum sample were calculated for relevant antigens on the microarray. For Jo-1, TPO, ssDNA, Ribo P, RNP, Smith, and La the relevant antigens are the same as the sera named. Relevant antigens for centromere include CENP-A and CENP-B; for mitochondrial include α-ketoglutarate dehydrogenase and pyruvate dehydrogenase; and for histone include histones H1, H2a and H4, H2b, and H3. (B) Titration of the ribo P-specific human positive control serum on FAST slides revealed decreasing fluorescence of ribo P and other positive antigens with higher dilutions of the sample. All microarrays were probed with Cy3-conjugated GAH IgG and IgM secondary antibody (Jackson ImmunoResearch Laboratories) at 1:2000 except for a control microarray with no secondary added. Antigens were printed in replicates of eight. For (A), each human positive control sera data point represents the median CV for eight replicates of all representative antigens on one microarray and the median data point represents the median of CVs for the 11 different sera. For Fig. 2B, each data point represents the median of eight replicate features on one microarray. RNP, ribonuclear protein.

formed better than FAST slides in their study printing HSA with solid pins and probing with a mAb. There are several possible explanations for why FAST slides did not perform as well in their studies including the difference in pin type used to produce the arrays. However, members of our laboratory have used solid pins for printing autoantigen microarrays and have found CVs similar to those reported in our study. The discrepancy in FAST performance is more likely due to differences in washing conditions or changes made in the FAST surface since the Angenendt study was undertaken. In

our studies, the performance of poly-L-lysine slides was quite variable depending on antigen type and concentration. Therefore, it is difficult to directly compare our results to the Angenendt study since we did not analyze the same antigen–antibody interaction. Finally, our laboratory has developed a two-color approach using FAb fragments to allow comparison of two samples on one microarray [15]. This technique improves reproducibility and the capacity to detect differences in antibody concentrations and isotype levels, thus providing an alternative approach to autoantigen microarray studies.

These studies demonstrate that FAST, PATH, and SuperEpoxy2 slides are all suitable for fabricating autoantigen microarrays. Overall, FAST slides had the lowest CV while maintaining excellent S/N. Our laboratory currently uses FAST slides for autoantigen microarray studies. However, depending on the antigen of interest and the types of analyses to be performed, PATH or SuperEpoxy2 slides may be more suitable. After optimizing the major variables in our current autoantigen microarray platform we are confident that the variance within and among microarrays is low enough to allow for detection of subtle differences within a patient over time and among patients. Ultimately such studies will be used to better understand disease pathogenesis, monitor patients' responses to therapy, determine prognosis, and develop antigen-specific therapies.

We thank the members of the Utz laboratory for their thoughtful discussions. I. B. is funded by an Arthritis Foundation Postdoctoral Fellowship. J. D. T. was funded by a fellowship from the National Library of Medicine as a Bioinformatics graduate student at Stanford University and is currently a Project Leader at the Duke Translational Medicine Institute at Duke University. P. J. U. is the recipient of a Donald E. and Delia B. Baxter Foundation Career Development Award, and was supported by the Dana Foundation, the Floren Family Trust, the Northern California Chapter of the Arthritis Foundation, NIH Grant AI051614 and NHLBI Proteomics Contract N01-HV-28183.

Conflict of interest statement: In the past 3 years P. J. U. has served as a consultant to Centocor (Horsham, PA), Biogen/Idec (Cambridge, MA), Avanir, Inc (La Jolla, CA), Astra Zeneca (London, UK), and Genentech (South San Francisco, CA). He is a member of the Scientific Advisory Board of Monogram Biosciences (South San Francisco, CA) and XDx (South San Francisco), and a cofounder and consultant at Bayhill Therapeutics (Palo Alto, CA). I. B., C. L., and J. D. T. have declared no conflict of interest.

References

[1] Balboni, I., Chan, S. M., Kattah, M., Tenenbaum, J. D. *et al.*, Multiplexed protein array platforms for analysis of autoimmune diseases. *Annu. Rev. Immunol.* 2006, *24*, 391–418.

[2] Robinson, W. H., DiGennaro, C., Hueber, W., Haab, B. B. *et al.*, Autoantigen microarrays for multiplex characterization of autoantibody responses. *Nat. Med.* 2002, *8*, 295–301.

[3] Feng, Y., Ke, X., Ma, R., Chen, Y. *et al.*, Parallel detection of autoantibodies with microarrays in rheumatoid diseases. *Clin. Chem.* 2004, *50*, 416–422.

[4] Li, Q. Z., Xie, C., Wu, T., Mackay, M. *et al.*, Identification of autoantibody clusters that best predict lupus disease activity using glomerular proteome arrays. *J. Clin. Invest.* 2005, *115*, 3428–3439.

[5] Li, Q. Z., Zhou, J., Wandstrat, A. E., Carr-Johnson, F. *et al.*, Protein array autoantibody profiles for insights into systemic lupus erythematosus and incomplete lupus syndromes. *Clin. Exp. Immunol.* 2007, *147*, 60–70.

[6] Hueber, W., Kidd, B. A., Tomooka, B. H., Lee, B. J. *et al.*, Antigen microarray profiling of autoantibodies in rheumatoid arthritis. *Arthritis. Rheum.* 2005, *52*, 2645–2655.

[7] Hueber, W., Tomooka, B. H., Zhao, X., Kidd, B. A. *et al.*, Proteomic analysis of secreted proteins in early rheumatoid arthritis: Anti-citrulline reactivity is associated with upregulation of proinflammatory cytokines. *Ann. Rheum. Dis.* 2007, *66*, 712–719.

[8] Quintana, F. J., Hagedorn, P. H., Elizur, G., Merbl, Y. *et al.*, Functional immunomics: Microarray analysis of IgG autoantibody repertoires predicts the future response of mice to induced diabetes. *Proc Natl. Acad. Sci. USA* 2004, *101*, 14615–14621.

[9] Robinson, W. H., Fontoura, P., Lee, B. J., De Vegvar, H. E. *et al.*, Protein microarrays guide tolerizing DNA vaccine treatment of autoimmune encephalomyelitis. *Nat. Biotechnol.* 2003, *21*, 1033–1039.

[10] Kanter, J. L., Narayana, S., Ho, P. P., Catz, I. *et al.*, Lipid microarrays identify key mediators of autoimmune brain inflammation. *Nat. Med.* 2006, *12*, 138–143.

[11] Lueking, A., Huber, O., Wirths, C., Schulte, K. *et al.*, Profiling of alopecia areata autoantigens based on protein microarray technology. *Mol. Cell. Proteomics* 2005, *4*, 1382–1390.

[12] Horn, S., Lueking, A., Murphy, D., Staudt, A. *et al.*, Profiling humoral autoimmune repertoire of dilated cardiomyopathy (DCM) patients and development of a disease-associated protein chip. *Proteomics* 2006, *6*, 605–613.

[13] Angenendt, P., Glokler, J., Sobek, J., Lehrach, H., Cahill, D. J., Next generation of protein microarray support materials: Evaluation for protein and antibody microarray applications. *J. Chromatogr. A* 2003, *1009*, 97–104.

[14] Haab, B. B., Dunham, M. J., Brown, P. O., Protein microarrays for highly parallel detection and quantitation of specific proteins and antibodies in complex solutions. *Genome Biol.* 2001, *2*, Research0004.0001–0004.0013.

[15] Kattah, M. G., Alemi, G. R., Thibault, D. L., Balboni, I., Utz, P. J., A new two-color Fab labeling method for autoantigen protein microarrays. *Nat. Methods.* 2006, *3*, 745–751.

